

3-Dimensional quantitative analysis of mandibular motion in TMD and healthy subjects: Comparison with clinical observations

Wen Tang^{a,b,c,1}, Yue Wu^{a,b,c,1}, Jiajun Ma^d, Peter Svensson^{e,f,g},
Kelun Wang^{g,h}, Hengjia Zhangⁱ, Lizhe Xie^{b,c,*}, Bin Yan^{a,b,c,*}

^a Department of Orthodontics, The Affiliated Stomatological Hospital of Nanjing Medical University, Gulou District, Nanjing, China

^b Jiangsu Key Laboratory of Oral Diseases, Nanjing Medical University, Nanjing, China

^c Jiangsu Province Engineering research of stomatological Translational Medicine, Nanjing Medical University, Gulou District, Nanjing, China

^d School of Cyber Science and Engineering, Southeast University, Nanjing, China

^e Faculty of Dentistry, National University of Singapore, Singapore

^f Faculty of Odontology, Malmö University, Malmö, Sweden

^g Sino-Denmark Orofacial Pain & TMD Research Unit, The Affiliated Stomatological Hospital of Nanjing Medical University, Nanjing, China

^h Center for Sensory-Motor Interaction (SMI), Aalborg University, Aalborg, Denmark

ⁱ Charles Clifford Dental Hospital, School of Clinical Dentistry, University of Sheffield, Sheffield, United Kingdom

ARTICLE INFO

Keywords:

Mandibular motion trajectory
Mandibular kinematic
Temporomandibular disorder
Jaw tracking system
Cone-beam computed tomography

ABSTRACT

Objectives: To establish a quantitative method for objectively assessing 3-dimensional (3D) mandibular trajectories and comparing clinical evaluations with computational analyses.

Methods: In total, 184 volunteers were recruited and grouped into control ($n = 121$) and temporomandibular disorder (TMD) groups ($n = 63$) according to the dual-axis DC/TMD checklist. 3D trajectories were generated by integrating mandibular motion and cone beam computed tomography (CBCT) records. Via digitalized data processing, the following 3 outcomes were assessed: (1) smoothness using the best-fitting polynomial curve, (2) open-closure separation by measuring the deviation between open-closure phases, and (3) condylar trajectory symmetry by comparing left and right movements. Intraclass Correlation Coefficients (ICC) were used to determine agreement between expert observations and quantitative results. Reference ranges for each parameter from the normal population were calculated. Mann–Whitney test was used to analyze the features of the trajectories between the two groups.

Results: ICC confirmed strong consistency between the parametric variations and expert observations (smoothness: 0.797; open-closure separation: 0.820; left-right symmetry: 0.920). Quantitative analyses revealed significant differences ($P < 0.043$ for smoothness, $P < 0.01$ for separation, and $P = 0.012$ for symmetry) in all comparisons between movement trajectories of normal participants and those with TMD, with the latter group exhibiting greater variation and irregularities. The normal range of smoothness was calculated for condylar trajectories between 0 and 0.25 and 0–0.10 for incisal point trajectories. Open-closure separation normal range was computed between 0 and 2.28 mm for incisal point trajectory, 0–1.90 mm for left condylar trajectory, and 0–1.76 mm for right condylar trajectory. The normal range of symmetry between condylar trajectories was calculated to be between 0 and 4.21 mm.

Conclusions: This quantitative analysis was confirmed to be reliable and consistent with expert observations. This allowed for the discovery of substantially quantified differences in smoothness, open-closure separation, and symmetry of the motion trajectories in TMD patients versus controls.

* Corresponding author at: Department of Orthodontics, The Affiliated Stomatological Hospital of Nanjing Medical University, Gulou District, Nanjing, China.
E-mail addresses: xielizhe@njmu.edu.cn (L. Xie), byan@njmu.edu.cn (B. Yan).

¹ Wen Tang and Yue Wu contributed equally as the first authors.

Clinical Significance

This study introduces a novel quantitative method for evaluating mandibular movements, which aids in diagnosing TMD and assessing treatment efficacy by quantifying trajectory features. By establishing standardized metrics and benchmarks alongside clinical examinations, this method might support the identification of individuals at risk for TMD or underlying pathological factors.

1. Introduction

The temporomandibular joint (TMJ) plays a pivotal role in performing various orofacial functions, including mastication, swallowing, and speaking [1]. Temporomandibular disorders (TMDs) are neuromuscular and musculoskeletal disorders affecting the TMJ and associated tissues. Epidemiological data indicate a high prevalence of TMDs, ranging from 30 %–50 % [2]. These conditions may provoke TMJ dysfunction, commonly manifested as irregularities in mandibular movement, joint sounds such as clicking, crepitus, and occasionally pain [3]. Thus, understanding the harmonized articular activity of TMJs, collectively known as mandibular movements, could be crucial for diagnosing and planning treatments for TMDs in patients troubled by their symptoms [4].

TMJ dysfunctions present unique diagnostic challenges due to their complex etiology and varied presentation [5]. The Dual Axis Diagnostic Criteria for Temporomandibular Disorders (DC/TMD) is the most comprehensive tool available for diagnosing TMD, encompassing both physical (Axis I) and psychosocial (Axis II) assessments [6]. However, it has been criticized for its complexity and research-oriented focus, which can complicate chairside application and lead to potential inconsistencies in diagnosis [7]. Clinical diagnosis of TMD is often challenging due to patient subjectivity, variability in the perception and presentation of TMD symptoms, and the lack of visible clinical or radiographic findings [8]. While magnetic resonance imaging (MRI) remains the gold standard imaging modality for evaluating TMJ soft tissue, it fails to capture the functional dynamics and motion-based aspects essential for a comprehensive understanding of TMJ disorders [9]. Clinicians frequently rely on qualitative assessment of movement trajectories to evaluate mandibular motion across various attributes [10]. Normal TMJ movements are characterized by smooth, symmetrical, superimposed trajectories, whereas dysfunctions, such as disc displacement with reduction (DDwR), exhibit irregular, non-overlapping paths [11,12]. These movement patterns are influenced by multiple biological factors, including muscles, ligaments, and the TMJ disc, which prevent exact superimposability between the right and left sides and introduce variability with each repetition [13]. This inherent variability complicates the visual assessment of mandibular motion trajectories for the clinical diagnosis of TMDs. Consequently, quantifying trajectory characteristics has become essential for accurately distinguishing pathological from normal mandibular movement, thereby enhancing clinical decision-making [14]. Treatment options for such irregularities range from no intervention to non-invasive management, with decisions guided by the patient's functional disability and the potential risk of adverse effects.

The lack of replicable and transparent quantification methods raises many predicaments. First, functional examination of the TMJ is susceptible to the influence of clinician subjectivity and individualized proficiency, resulting in diagnostic inconsistencies and poor repeatability. Second, considering the need for reference standards to compare different results from different devices, the absence of generalizable benchmarks for functional assessment of the TMJ poses a significant clinical challenge. Third, the dearth of robust quantifiable diagnostic

biomarkers imperils the proper monitoring of TMD progression and the efficacy of various therapeutic modalities, hindering the implementation of further evidence-based treatment optimizations. Finally, there is a pressing demand for retrospective or prospective cohort experiments to provide baseline data for further development of reliable artificial intelligence (AI)-based assessments. Therefore, conducting well-designed case-control studies is imperative to make methodological comparisons and increase the level of evidence regarding the clinical significance of mandibular kinematics [10].

Various methods have been employed to generate movement trajectories to assess TMJ functionality. While CADIAX—a classic mechanical device—is renowned for its commendable accuracy, it struggles with reconstructing three-dimensional (3D) trajectories to depict condylar movement [12]. Ultrasound and optical tracking systems, such as Zebris, Modjaw, and SDiMatrix, have demonstrated promising performance in capturing 3D trajectories [15–17]. Optical tracking systems can record mandibular motion at high speeds and offer greater precision than ultrasound devices, thereby providing additional opportunities for digital analytics [18]. With remarkable advancements in acquisition technologies, current studies have primarily focused on quantitative analyses of parameters such as the range of the movement, condylar guidance inclination, and incisal guidance inclination [18,19]. Moreover, previous evaluations of trajectory smoothness and symmetry have mostly been based on two-dimensional trajectories [20–22], which are susceptible to errors due to the influence of projection direction. This can lead to inconsistencies in diagnoses among observers. Additionally, such approaches may fail to accurately reveal subtle abnormalities in mandibular movements, resulting in misdiagnoses or missed diagnoses. Overall, there is still a lack of unified and reliable standards for quantitative evaluation methods of movement smoothness, left-right symmetry and open-closure separation of three-dimensional motion trajectories.

This study aimed to develop an innovative, multifaceted, and quantitative approach for characterizing mandibular movement. We aimed to demonstrate the consistency and reliability of this quantification method by comparing expert clinical assessments with computer-generated quantitative results. This approach aims to be applicable to data from various mandibular motion devices, potentially facilitating the objective diagnosis of TMJ movements and enhancing the functionality of existing diagnostic tools. Specifically, we propose a computational data-processing method to quantify the smoothness, separation, and symmetry of mandibular movements, thereby providing novel insights into clinical examinations.

2. Materials and methods

2.1. Participants

This cross-sectional study included 184 volunteers with stable occlusion (excluding third molars) and no history of craniofacial trauma, systemic diseases, orthodontic treatment, major maxillofacial surgery, or full/partial denture wear. Participants were divided into control ($n = 121$; mean age 24.8 years with 76 females) and TMD ($n = 63$; mean age: 27.2 years with 43 females) groups based on the DC/TMD checklist [6], clinical examination, and magnetic resonance imaging (MRI). Control group participants met the following criteria to confirm the acceptability of their bialveolar interdigitation and occlusion:

- 1) Aged between 20 and 30 years
- 2) Complete natural permanent dentition (excluding the third molars)
- 3) Class I occlusion without crossbite
- 4) Maximum mouth opening distance > 40 mm
- 5) CR-CO (Centric relation-centric occlusion) discrepancies of < 2 mm in all directions
- 6) No clicking sound at the TMJ
- 7) No significant mandibular lateral deviations during mouth opening

8) No joint and/or muscle tenderness

Three clinicians specializing in TMD and orofacial pain independently evaluated and categorized the participants and were blinded to each other's diagnoses. This study adhered to the Strengthening The Reporting of Observational Studies in Epidemiology (STROBE) checklist for observational studies, ensuring comprehensive and transparent reporting of our methodology and findings [23]. Ethical approval was granted by the National Clinical Trial Registry (Identifier ChiCTR23000772980) and the Ethics Committee of Stomatology Hospital (PJ2022-110-001). After fully understanding the study elements and procedures, all participants provided written informed consent. Fig. 1A shows a flowchart of the study procedures.

2.2. Data acquisition

This study used a joint motion acquisition and analytical device developed in collaboration with an external company (Nanjing Medical and Industrial Cross Innovation Research Institute Co., Ltd). To create a 4D mandibular kinetic representation, we separately collected motion data from our self-developed binocular stereo vision system (BSVS) (Prototype, Nanjing Medical and Industrial Cross Innovation Research Institute Co., Ltd, P.R. China) and morphological data from the cone-beam computed tomography CBCT (Fig. 1B: Step 1). The BSVS, operating at a frequency of 20 Hz, utilized a binocular acquisition system comprising two industrial cameras (Daheng Imaging, Beijing, China). Videos were captured at 2048(H) x 1536(V) resolution and 20 fps, with the system software performing tasks such as camera calibration (to avoid the influence of nonlinear distortions), image acquisition, stereo matching, and 3D reconstruction. Jaw trackers with targeted markers and embedded metallic sensors were delicately bonded to the intraoral facial surfaces of the upper and lower teeth via T-attachments without soft tissue alterations or occlusal disturbances during rest or functional positions (Supplementary File 1, Figure S2). The midline of the T-attachment was confirmed to coincide with the facial midline and bonded parallel to the occlusal plane from the first premolars on the left to right. All marked points were confirmed to reside clearly and utterly visible within the field of vision for both the binocular stereo system and CBCT.

The participants performed a customary cycle of unguided, pain-free, maximum jaw open-closure, starting and ending at maximum intercuspation. Verbal instructions were provided to all participants. Three trial attempts preceded the final execution of accurate data collection. The participants were allowed ample rest and therapeutic manoeuvres to mitigate likely errors due to muscle contracture. CBCT scans (VGi; voxel size: 0.3 mm, field of view: 16 × 16 cm; NewTom, Imola, Italy) were uniformly obtained using the same positioning protocol. The region-growing-based segmentation method was used for 3D reconstruction of the jaws. All examinations and procedures were performed by the same operators (TW and WY).

2.3. Motion reconstruction

Multimodal data fusion was conducted using the BSVS software, integrating static 3D CBCT images with dynamic occlusion data by matching them at a specific time frame. The motion matrices of targeted points were aligned with the reconstructed maxilla and mandible using the iterative nearest-point method, ensuring consistent alignment and optimal transformation [24]. The pyramid Lucas-Kanade optical flow method was applied to mitigate errors from velocity variations, thereby enhancing the robustness of the motion matrices [25]. After CBCT region-growing-based segmentation, motion matrices were mapped between the 3D world and CBCT coordinate systems by automatically recognizing embedded metallic sensors that were visible in both visual and CT acquisition phases. Following this established and refined coordinate mapping, we merged the 3D reconstructed static feature

information with the motion matrices to visualize the mandibular movement relative to the maxillary apparatus. To ensure computational accuracy, the entire motion matrix sequence was nonlinearly optimized considering the Markovian nature of TMJ motion, thus minimizing systematic errors [26].

For motion reconstruction, MeVisLab software (MeVis Medical Solutions, Bremen, Germany) was used to process and identify landmarks using CBCT images. The scans were reoriented such that The XOY plane corresponded to the Frankfort horizontal plane, and the Z-axis was aligned perpendicular to both planes. Three reference points (bilateral condylar centers and lower incisal points) were manually identified, and their 3D coordinates were verified for consistency in different planes, rendering 3D motion trajectories. The mean values of the 3D coordinates were used by BSVS software to generate three motion trajectories and matrices on merged 4D records (Fig. 1B: Step 2). One examiner (TW) repeated the process in two rounds with a one-week interval to ensure reliability.

2.4. Quantitative data processing

The three parameters to be explained are identified and illustrated in Fig. 2. Motion matrices were used to obtain displacement data for all reference points. We applied preprocessing measures to account for variations in movement velocity among subjects during data collection (Supplementary File 1).

Smoothness: Irregularities or tremors in mandibular movement were taken as indications of a non-smooth movement. The motion trajectory was segmented into opening and closing phases by identifying the maximum displacement point. The coefficient of determination (R^2) was introduced to explain the smoothness of the trajectory curve. To ensure consistency among all quantification parameters, we defined TSm as $1 - R^2$, calculated as Eq.(3). Hereby, SST (Eq.(1)) is the total sum of squares, X_i , Y_i and Z_i are the coordinate values at the i^{th} time point during movement; and, \bar{X} , \bar{Y} and \bar{Z} signify the mean coordinate values across all the recorded frames. \hat{X} , \hat{Y} and \hat{Z} are the coordinate values of the predicted time points throughout the best-fitted curve. The residual sum of squares (SSE) was determined by Eq. (2). The TSm value, derived from the ratio of SSE to the SST as yielded via Eq. (3), serves as the final metric for trajectory smoothness (ranging from 0 to 1), with lower values indicating smoother trajectories.

$$SST = \sum_{i=1}^n ((X_i - \bar{X})^2 + (Y_i - \bar{Y})^2 + (Z_i - \bar{Z})^2) \quad (1)$$

$$SSE = \sum_{i=1}^n ((X_i - \hat{X}_i)^2 + (Y_i - \hat{Y}_i)^2 + (Z_i - \hat{Z}_i)^2) \quad (2)$$

$$TSm = 1 - R^2 = \frac{SSE}{SST} \quad (3)$$

Open-closure Separation: The concordance extent between the opening and closing segments of mandibular movement provides insights into the normal functioning and potential disorders of the jaw. The lock-step Euclidean distance was used to calculate the separation of opening and closing trajectories based on the maximum displacement point. Considering the asynchrony and temporal sequencing, the dynamic time warping algorithm is used to match trajectory points [27]. The Euclidean distances projected in three axes quantified the separation between the opening (o) and closing (c) segments, as determined by Eq. (4), where n denotes the total number of juxtaposed time points. Lower mean Euclidean distances indicated less separation (TSp) between movement phases (Fig. 3D).

$$TSp = \frac{\sum_{i=1}^n \sqrt{(x_o - x_c)^2 + (y_o - y_c)^2 + (z_o - z_c)^2}}{n} \quad (4)$$

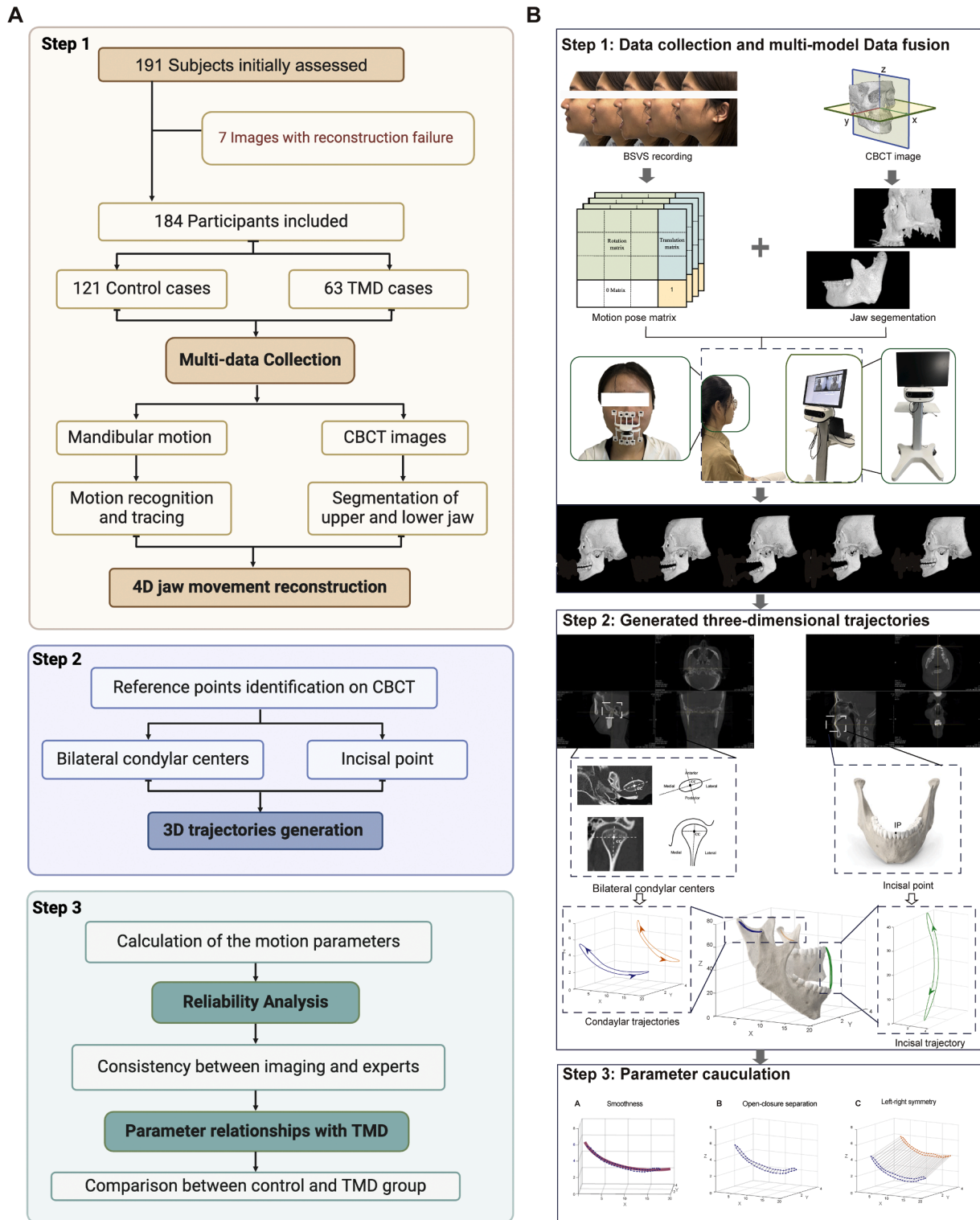


Fig. 1. Study protocol. (A) Summarized flow chart of the methodological procedures corresponding to the diagrammatic presentation. (B) Step-by-step diagrammatic representation of motion trajectory generation. (Step 1) Recording mandibular movement using BSVS and CBCT images, followed by fusion of CBCT and BSVS footages of mandibular open-closure movements and jaw motion video reconstruction in BSVS image manipulation software. (Step 2) Generation of the reference points' movement trajectories in the Python software. The intersection points of the mediolateral, anteroposterior, and superoinferior axes, confirmed in the axial and coronal planes, were denoted as the left condyle center (LCC) and right condyle center (RCC), respectively. The incisal point (IP) was marked in CBCT. (Step 3) The calculation of three variables in mandibular movement trajectories.

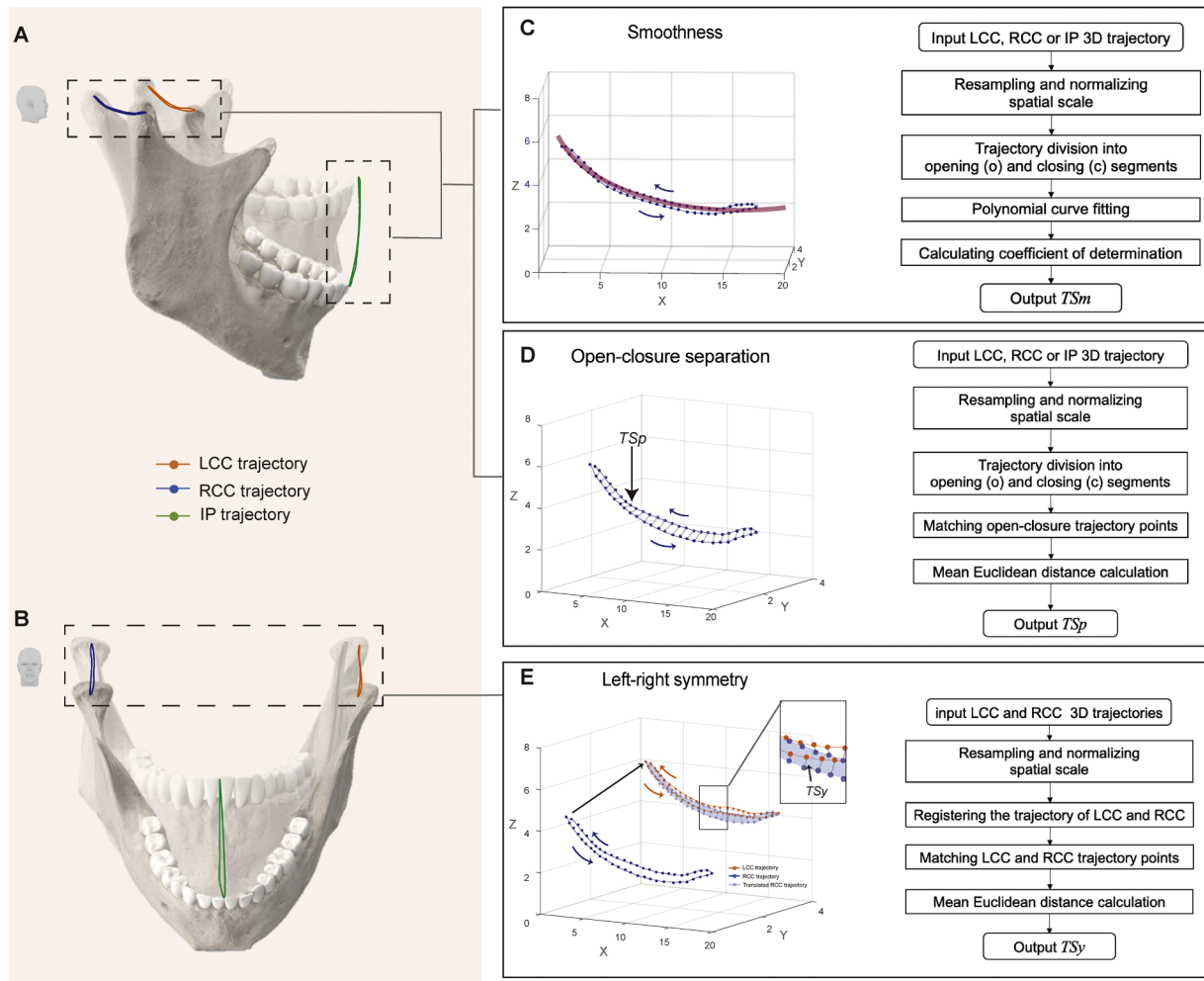


Fig. 2. Illustration of quantified variables in mandibular movement trajectories. (A, B) Sagittal and frontal mandibular view along with the delineated trajectories. (C) Smoothness (T_{Sm}), which measures the determination coefficient between the trajectories from the best-fitting polynomial curve. (D) Open-closure separation was measured between the opening and closing segments of each trajectory (T_{Sp}). (E) Left-right symmetry was calculated using measured distances between timepoint-matched points between the left and right condylar trajectories (T_{Sy}). Each addressed feature in the image is accommodated with its respective diagrammatic flow of the computational process.

Left-right Symmetry: The symmetry of mandibular movement was evaluated by quantifying the similarity of the movement trajectories of the left and right condylar centers (LCC and RCC) during the opening and closing process. The Euclidean distance was used to evaluate the symmetry of the condylar mandibular movements. After the initial point of the trajectory of the right condyle was translated to that of the left condyle, a time-point matching algorithm was employed to synchronize the kinematic profiles of the right condyle, enabling the quantification of mandibular motion symmetry. The mean Euclidean distances of the corresponding time points projected onto $X_{(l\&r)}$, $Y_{(l\&r)}$, and $Z_{(l\&r)}$ were measured using Eq. (5). A smaller T_S indicated more symmetrical condylar movements (Fig. 3E).

$$T_S = \frac{\sum_{i=1}^n \sqrt{(x_i - x_r)^2 + (y_i - y_r)^2 + (z_i - z_r)^2}}{n} \quad (5)$$

2.5. Reliability and qualitative analysis

Two separate well-experienced examiners (YB and LH) independently conducted the blinded visual scoring of the rendered 3D trajectories, with a third examiner (ZW) available to resolve disagreements if necessary. Smoothness was evaluated by categorizing motion paths as either "high smoothness" or "low smoothness". High smoothness

indicated uninterrupted, consistent motion paths, whereas low smoothness was characterized by noticeable zigzags and abrupt bends. The qualitative criteria used in this evaluation included uninterrupted curves with no breaks or pauses, smooth velocity transitions without abrupt accelerations or decelerations. The fulfillment of these criteria indicated high smoothness, whereas their absence was suggestive of low smoothness.

Separation between the open and closed trajectories was evaluated to assess the degree of spatial displacement during mandibular motion. "Highly separated" was defined as a substantial spatial displacement between the open and closed movement trajectories, with marked divergence and distance in space. The morphology and direction of the trajectories during opening and closing cycles were notably inconsistent. This level of separation indicates a pronounced divergence in the movement paths during these cycles, potentially reflecting underlying joint dysfunction or instability. In contrast, "less separated" was characterized by minimal spatial displacement between the open and closed trajectories, with paths that remained relatively close and highly consistent. The trajectories displayed no significant divergence or offset, suggesting well-coordinated mandibular motion.

Symmetry between the left and right condylar trajectories was evaluated to understand the degree of coordination in mandibular movements. This assessment was categorized into three distinct grades

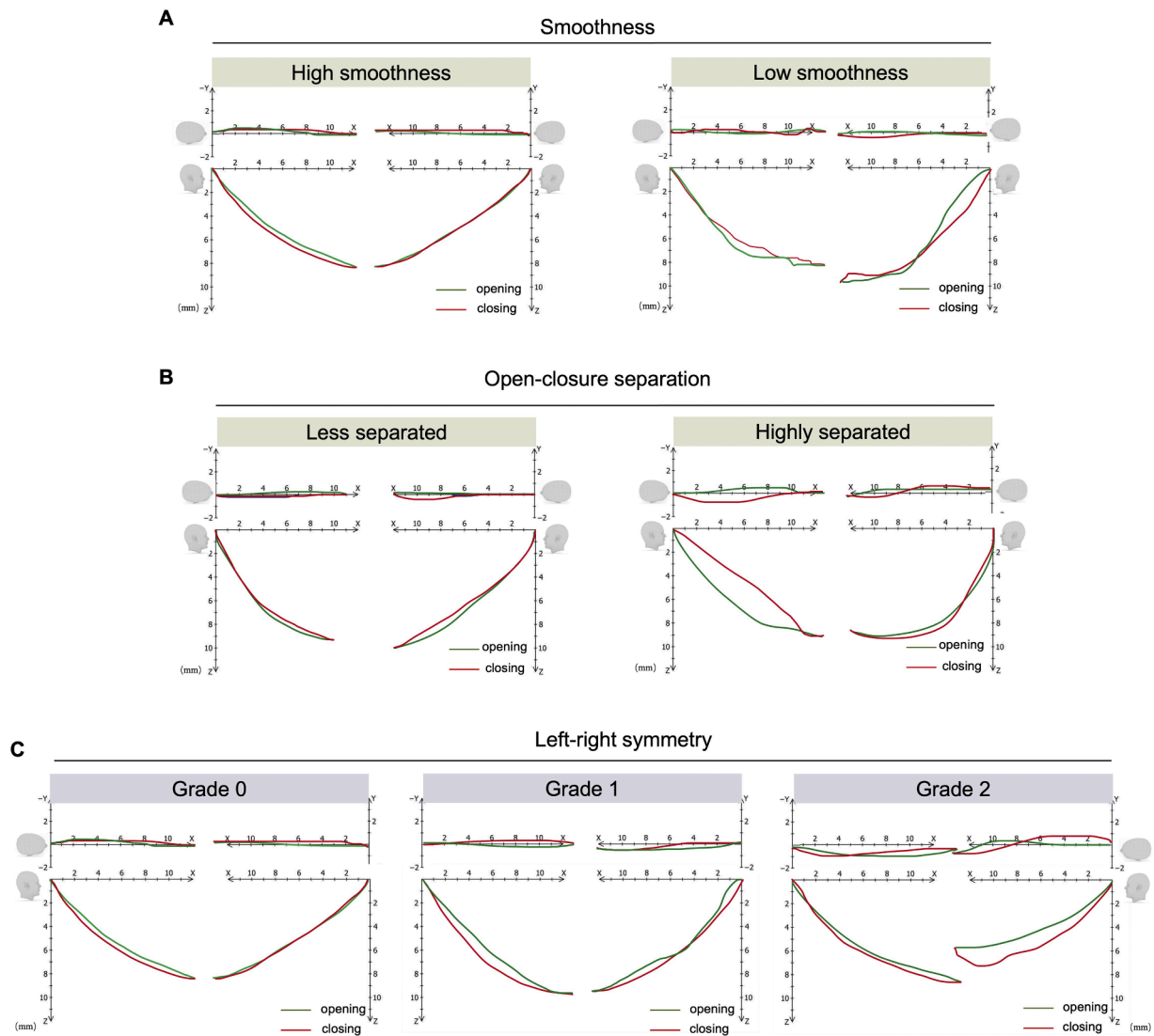


Fig. 3. Diagrammatic representation of expert criteria for qualitative analysis (A, B) The presence or absence of smoothness and Open-closure separation were visually assessed and determined to qualify the rendered trajectories. (C) The grading index of Left-right symmetry based on the shape resemblance and biplanar elongation comparison between the trajectories.

based on shape congruence and dimensional similarities. **Grade 0** symmetry was assigned to trajectories exhibiting high congruence in shape and dimensional similarity, with discrepancies <1 mm in both the Y (vertical) and Z (anteroposterior) dimensions. **Grade 1** symmetry encompassed trajectories that displayed differences in shape but maintained dimensional discrepancies of <1 mm, or showed biplanar length differences greater than 1 mm while retaining overall shape resemblance. **Grade 2** symmetry was characterized by concurrent configurational (shape) and dimensional disparities between the trajectories. Significant differences in both the form and dimensions of the condylar paths indicate pronounced asymmetry of mandibular movements in the eyes of examiners.

2.6. Statistical analysis

A minimum of 60 participants per group was recommended by G-power 3.1.2 (Heinrich-Heine-Universität Düsseldorf, Düsseldorf, Germany) to ensure 90 % power for the actual sample size. Statistical analyses were conducted using Python v3.7.1 (Python Software Foundation, Delaware, US). The weighted Cohen's kappa test was used to determine the intraobserver consistency of the expert scores.

Descriptive statistics were calculated, and listwise deletion was employed to exclude cases with missing data. Intraclass correlation coefficient (ICC) analysis was conducted to ensure the intraexaminer reliability of motion reconstruction. ICC analysis was also used to assess the agreement between the experts' observations and the quantitative results, with the significance level set at $P < 0.05$. The Shapiro-Wilk and Levene's tests were performed to assess normality and homogeneity of variance. Based on the normality results, the Mann-Whitney U test was used due to the non-normal distribution of the data. The 95th percentile (P95) was calculated to determine the reference range for each parameter in the healthy population.

3. Results

3.1. Reliability and concordance results

The ICC values for the coordinates of the reference points along the X, Y, and Z axes were 0.983, 0.978, and 0.937, respectively, indicating strong intra-examiner agreement in the measurements. Additionally, Cohen's kappa coefficient (κ) was calculated to be 0.87, demonstrating robust interobserver agreement among the examiners. A detailed

Table 1
Frequency of expert qualitative assessments regarding each parameter in both Groups.

Parameters		Grade	Normal (n = 121)	TMD (n = 63)	χ^2	P		
Smoothness	IP-open	Low smoothness	27	20	1.938	0.164		
		High smoothness	94	43				
	LCC-open	Low smoothness	42	29	2.241	0.134		
		High smoothness	79	34				
	RCC-open	Low smoothness	38	32	6.608	0.010*		
		High smoothness	83	31				
	IP-close	Low smoothness	25	12	0.067	0.796		
		High smoothness	96	51				
	LCC-close	Low smoothness	37	27	2.753	0.097		
		High smoothness	84	36				
	RCC-close	Low smoothness	30	34	15.545	<0.001*		
		High smoothness	91	29				
	IP-total	Low smoothness	26	22	3.877	0.049*		
		High smoothness	95	41				
	LCC-total	Low smoothness	46	32	2.770	0.096		
		High smoothness	75	31				
	RCC-total	Low smoothness	44	30	2.183	0.140		
		High smoothness	77	33				
	Open-closure separation	IP	Highly separated	98	24	34.122	<0.001*	
			Less separated	23	39			
		LCC	Highly separated	89	31	10.826	0.001*	
			Less separated	32	32			
		RCC	Highly separated	93	34	10.153	0.001*	
			Less separated	28	29			
		Left-right symmetry	Grade 0		53	15	11.552	0.002*
			Grade 1		64	19		
			Grade 2		4	29		

* indicates a significant difference ($P < 0.05$).

breakdown of each examiner's categorical assessments regarding trajectory attributes is provided in Table S5. Table 1 presents the comparison between the qualitative expert evaluations of the mandibular motion trajectories in two groups. ICC analysis revealed a significant association between the quantitative measurements of the mandibular motion trajectories and the observations made by the experts. Specifically, the ICC values were 0.797 for smoothness, 0.820 for open-closure separation, and 0.920 for left-right symmetry (Table 2), indicating high reliability in these assessments. Fig. 4 presents a schematic diagram to show the consistency and linkage between expert observation of clinical performance and the three aspects of the 3D quantitative analysis.

3.2. Intergroup comparisons

Of the 191 potentially eligible participants, seven were excluded due

Table 2
Results of the ICC analysis of expert clinical scores and the quantification outcomes.

Parameters		ICC value	
Smoothness	IP-open	0.782	0.797
	LCC-open	0.817	
	RCC-open	0.752	
	IP-close	0.820	
	LCC-close	0.743	
	RCC-close	0.745	
	IP-total	0.772	
	LCC-total	0.748	
	RCC-total	0.738	
Open-closure separation (mm)	IP	0.809	0.820
	LCC	0.813	
	RCC	0.802	
Left-right symmetry (mm)		0.920	0.920

to unsuccessful image reconstruction, resulting in a final sample size of 184 individuals. The descriptive statistics and distribution patterns of all measured variables are presented in Table 3. Quantitative analysis effectively identified a significant difference between the control and TMD groups. The 95th percentile (P95) results were used to define the normal ranges, indicating that 95 % of the parameter values in the normal population fell within these ranges. The normal range of smoothness was calculated to be between 0 and 0.25 for condylar trajectories and between 0 and 0.10 for incisal point trajectories. The normal range for open-closure separation was computed as 0–2.28 mm for incisal point trajectories, 0–1.90 mm for left condylar trajectories, and 0–1.76 mm for right condylar trajectories. The normal range of symmetry between condylar trajectories was calculated to be between 0 and 4.21 mm. Parameters exceeding these normal ranges suggested a higher probability of TMD (Table 4).

As shown in the frequency plot, the TMD group exhibited a greater degree of standard deviation (SD) regarding smoothness, indicating greater variability. Furthermore, the control group demonstrated significantly greater smoothness than the TMD group (Fig. 5A, E). Regarding open-closure separation, the TSp values were significantly lower in the normal participants than in the TMD participants across all trajectories. The frequency distribution diagram revealed a more discrete distribution of measurements in the TMD group regarding this variable (Fig. 5B). Additionally, the SDs were significantly greater for the separation of open-closure trajectories in the TMD group (Fig. 5F). For symmetry of the condylar trajectories, the bar chart indicates a statistically significant difference ($P < 0.05$) between the two groups, with smaller TSy values observed in the control group. The frequency distribution chart also revealed a greater SD in the TMD group, which is consistent with the skewed data distribution observed in this group regarding other parameters (Fig. 5C, D).

4. Discussion

This study marks the initial attempt to quantify multiple aspects of 3D jaw motion trajectories. In line with expert evaluations, parameters such as smoothness, open-closure separation, and left-right symmetry proved to be reliable indicators for the functional assessment of mandibular movement. Additionally, the 3D quantitative analysis of mandibular may benefit various dental and medical applications. It can assist in orthodontic diagnosis and treatment planning, prosthodontic design of dental prosthetics, orthognathic surgery for pre- and post-surgical evaluations, and maxillofacial trauma assessment and rehabilitation. These findings underscore the broad clinical utility of 3D mandibular motion analysis across multiple disciplines [28–31]. We comprehensively analyzed mandibular movement in normal individuals and those with MRI-verified anterior disc displacement and identified substantial differences between them. Our findings imply that

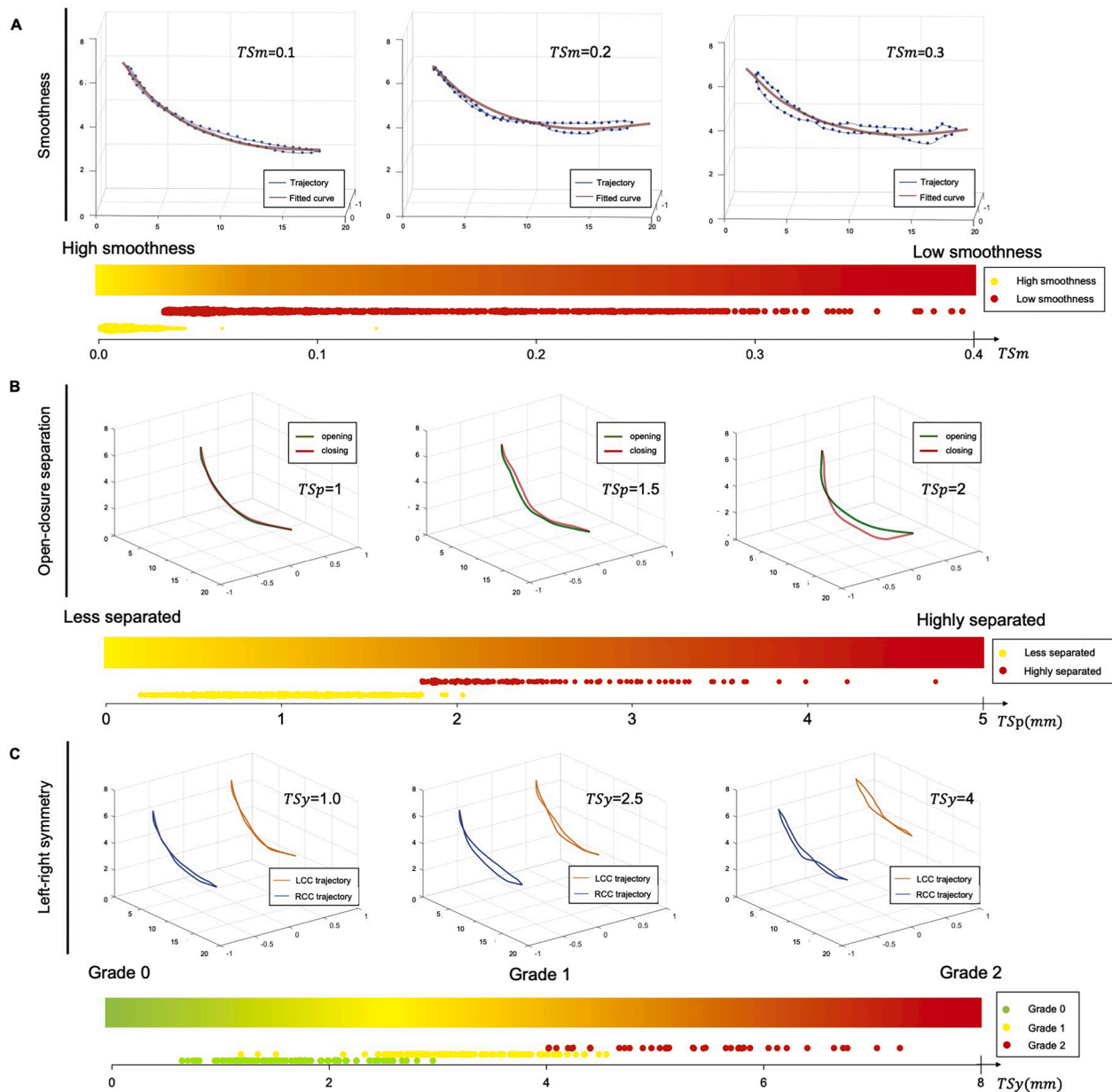


Fig. 4. Schematic visualization of mandibular motion trajectory parameters. Each parameter diagram consists of clinical examples of rendered trajectories, a color bar indicator of respective quantitative indicators, and a scatter plot below each parameter to illustrate the distribution patterns. (A) Smoothness (T_{Sm}): Lower T_{Sm} values correspond to smoother trajectories, degrading from the yellow part of the color bar (high smoothness) to red (low smoothness) as the T_{Sm} value increases. The transition coincides with the clinical observation of the above trajectories. (B) Open-closure separation (T_{Sp}): Greater separation is indicated by increasing T_{Sp} values, with a gradient from yellow (less separated) to red (highly separated) side of color bar. (C) Left-right symmetry (T_{Sy}): Symmetry decreases with increasing T_{Sy} values, shown by a shift from green (Grade 0) to yellow (Grade 1) and red (Grade 2).

quantifying diverse indicators is a promising method for distinguishing patients with TMD from normal individuals. As incisor and condylar motion ranges are crucial diagnostic criteria for TMJ disorders in the DC/TMD checklist, the condylar centers and incisal points served as reference landmarks [6]. The data processed in this study were obtained from an unguided maximum open-close cycle, a method previously employed for functional adjustments in prosthodontics and TMD screening [32]. Maximal intercuspation was adopted as the stable occlusal position at each cycle initiation and termination for the dynamic biomechanical mandibular analyses [33]. To optimize the accuracy of the tracing and registration processes, this study employed a highly controlled experimental design characterized by repetitive movements, averting soft tissue interference and assuring firm fixation of devices to the teeth. The samples were carefully selected to ensure as

much homogeneity as possible, minimizing the potential influence of variables such as age and TMD severity on the results [34]. Some research indicates that male subjects have a significantly higher maximum mouth opening than female subjects [35], while other studies suggest minimal gender-related differences in mandibular movement trajectories [34]. Therefore, sexual predisposition was not a focal point in our investigation.

Conventional studies typically present results as point curves on a two-dimensional (2D) plane, which oversimplifies the complex six-degrees of freedom inherent in TMJ movements [12]. This approach constrains the calculation of the projection range and angle in three separate 2D planes, necessitating an arbitrary selection of a reference frame to derive 3D trajectory data, which introduces errors [36]. Although 2D planar analysis is intuitive for clinicians, its reliability is

Table 3
Presentation of descriptive analysis results and U test analysis.

Parameters		Normal	TMD	<i>P</i> value	
Smoothness	IP-open	0.012 (0.005, 0.028)	0.023 (0.007, 0.051)	0.003*	
	LCC-open	0.031 (0.015, 0.094)	0.083 (0.039, 0.142)	<0.001	
	RCC-open	0.043 (0.019, 0.110)	0.065 (0.026, 0.186)	0.026*	
	IP-close	0.011 (0.004, 0.021)	0.012 (0.006, 0.032)	0.043*	
	LCC-close	0.031 (0.015, 0.087)	0.105 (0.035, 0.260)	<0.001*	
	RCC-close	0.038 (0.015, 0.107)	0.065 (0.024, 0.118)	0.037*	
	IP-total	0.013 (0.006, 0.027)	0.019 (0.009, 0.045)	0.004*	
	LCC-total	0.040 (0.020, 0.124)	0.119 (0.045, 0.199)	<0.001*	
	RCC-total	0.043 (0.021, 0.127)	0.069 (0.036, 0.189)	0.007*	
	Open-closure separation (mm)	IP	1.305 (1.087, 1.717)	2.048 (1.228, 2.944)	<0.001*
		LCC	0.890 (0.601, 1.279)	1.538 (0.878, 2.162)	<0.001*
		RCC	0.849 (0.620, 1.352)	1.153 (0.797, 1.893)	<0.001*
Left-right symmetry (mm)		2.816 (1.732, 3.401)	2.818 (2.147, 5.452)	0.012*	

Data are expressed as median (interquartile range).
* indicates a significant difference ($P < 0.05$).

Table 4
The normal reference ranges of the parameters.

Parameters		Normal range
Smoothness	IP-open	0 ~ 0.082
	LCC-open	0 ~ 0.214
	RCC-open	0 ~ 0.247
	IP-close	0 ~ 0.095
	LCC-close	0 ~ 0.202
	RCC-close	0 ~ 0.221
	IP-total	0 ~ 0.089
	LCC-total	0 ~ 0.174
Open-closure separation (mm)	RCC-total	0 ~ 0.171
	IP	0 ~ 2.284
	LCC	0 ~ 1.899
Left-right symmetry (mm)		RCC 0 ~ 1.756 0 ~ 4.214

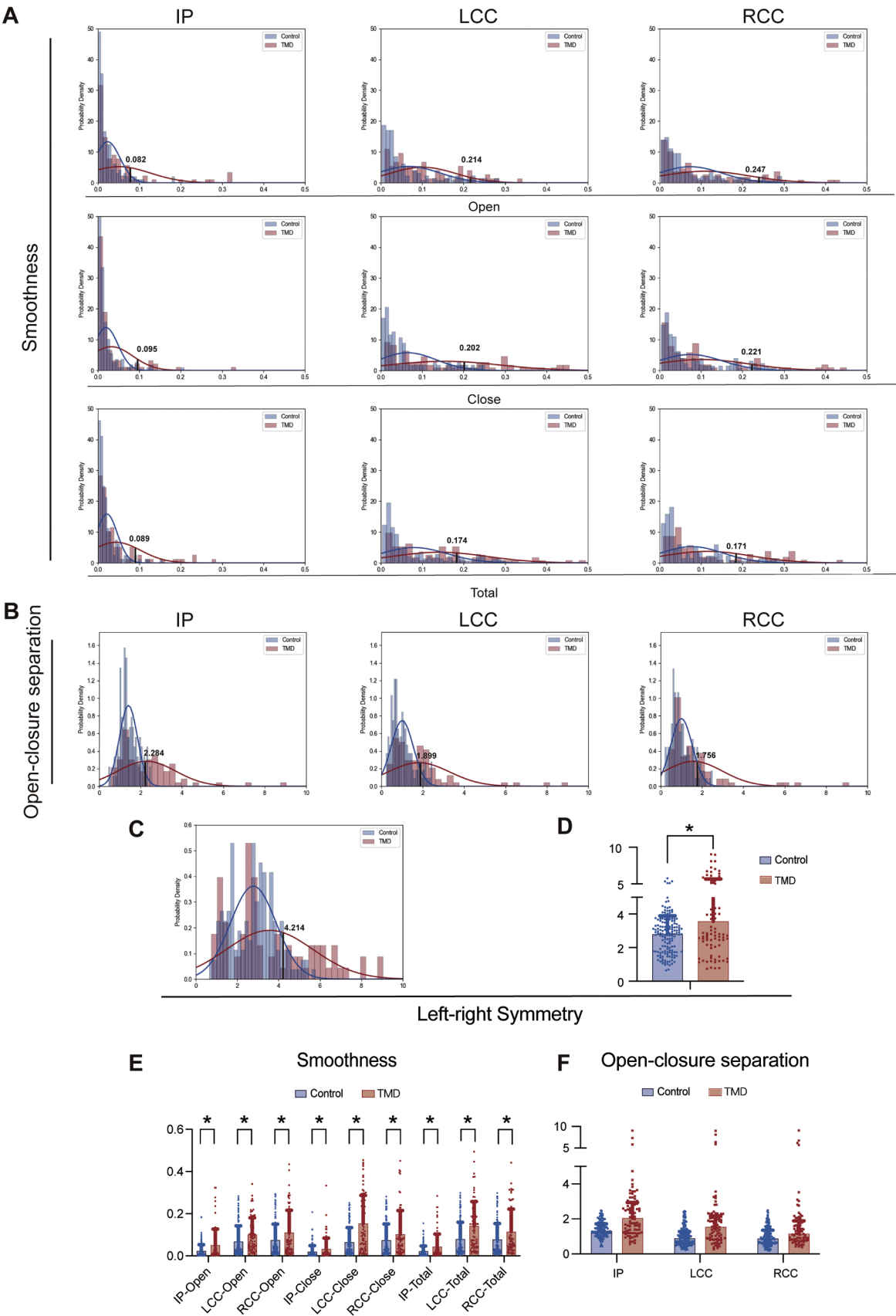
compromised because kinematic outcomes rely heavily on the choice of the reference frame [37]. Inconsistencies in defining the reference frame can lead to substantial interobserver discrepancies and conflicting diagnostic implications [38]. Previous investigations have reported controversial findings regarding the range of motion in patients with TMD [39]. Therefore, relying solely on the range of motion in clinical assessments might not conclusively distinguish abnormal condylar functioning, thereby overlooking the associated risks. The diverse ranges reported in previous studies and the likely impact of ethnicity emphasize the need for more refined techniques to establish normative data [40]. Achieving this goal effectively requires supplementing the analysis with a multifaceted and versatile quantification of trajectory characteristics.

Recent advancements in mandibular movement analysis have focused on evaluating acquired trajectories to gain deeper insights into TMJ dynamics. Traditionally, mandibular motion smoothness has been gauged by assessing the uniformity or irregularities in trajectory traces, with variability often observed due to subjective criteria across examiners [12]. Despite challenges in detecting subtle tremors, the overall

overlap of condylar trajectories in healthy subjects has also been well-documented, particularly in open-closure cycles. In contrast, patients with TMD exhibit abnormal mandibular patterns, such as deflections, erratic movements, and 8-shaped trajectories. These findings underscore the importance of refining trajectory-based analysis beyond subjective categorical methods that rely solely on visual observation. Although the smoothness and overlap of mandibular movements serve as crucial markers in TMJ examinations, their significance remains understudied, particularly compared with the detailed kinematic analyses of other joints [36,37]. Emerging technologies, such as high-resolution optical scanning systems like Zebris (Isny, Germany) and Modjaw (Villeurbanne, France), have facilitated more accurate tracking of jaw movement. Mandibular motion analysis can evolve into a more objective and reliable tool for functional TMJ assessment by incorporating quantitative parameters such as smoothness and separation. Our algorithm differentiated normal subjects from TMD cases by highlighting the reduced smoothness and separation in the latter group. Additionally, according to our descriptive findings, the smoothness of condylar trajectories in both groups decreased compared with inter-incisal point (IP) trajectories. This observation might be attributed to the geonatomical differences between the reference points, stressing the significance of intrajoint examinations to reflect more accurately the impacts of TMDs on mandibular movement.

The multiaxial TSy of the control group indicated greater symmetrical movement than that of the TMD group. Given its potential association with TMDs, analyzing asymmetries in mandibular movement is of paramount importance [40]. Lezcano et al. previously assessed mandibular movement symmetry in asymptomatic individuals, relying solely on the symmetry of Posselt polygons and 2D projection of reference planes, which is an imminent source of error [22]. Our study revealed the complexity of mandibular motion and symmetry by utilizing exposed individually diverted loci via 3D projection. Another alternative method employed MRI to objectively evaluate asymmetry, albeit with a limited sample size, possibly due to procedural inconvenience. Moreover, the generalizability of the authors' method for the consistent reproduction of customary mandibular movement is questionable when a neutral head position cannot be secured in an MRI machine, leading to conflicting and unreliable quantified data [41]. Although MRI remains the gold standard for TMJ soft tissue and disc-condyle relationship monitoring, CBCT-based 3D volumetric reconstruction yields superior quantitative data for bone or other hard tissue morphology assessments and is essential for training advanced AI algorithms [42].

From a clinical perspective, the differences between the control and TMD groups were related to statistically significant yet clinically minor increases in variation. Calculating the 95th percentile for each assessor helps clinicians determine and understand the normal reference range for quantitative indicators, thereby identifying values that are abnormally high or low values. This approach highlights deviations in the TMD group, emphasizing their clinical significance in the context of the normal distribution. Values outside this benchmark range may require further medical evaluation or intervention for the TMJ. This is helpful in establishing related diagnostic standards and health guidelines. The proposed quantitative method offers several significant clinical advantages. First, it enhances diagnostic accuracy by enabling clinicians to identify subtle clinical symptoms more precisely. Second, it facilitates the identification of high-risk populations by enriching the clinical perception of borderline TMJ symptomatic pathologies independent of practitioner expertise. Moreover, the variability of trajectory behaviour could be argued to be a signature or manifestation of the biomechanical and pathophysiological pathways leading to more severe symptoms. This method, therefore, has the potential to improve the diagnosis of patients with first-onset TMD, characterized by symptoms such as orofacial pain and jaw stiffness or soreness, thus enabling timely intervention. Furthermore, this parametric reflection of mandibular motion intricacies facilitates not only accurate, individualized pre- and



(caption on next page)

Fig. 5. Frequency data distribution histograms and comparative bar charts between study groups. (A) Smoothness data distribution of three different trajectories under different circumstances of the opening segment of the movement, the closing phase, and the total trajectory. (B) Distribution of measured data regarding the separation of open closure segments. (C) Frequency histogram of measured symmetry between bilateral condylar trajectories. (D) Bar chart of the statistical analysis between the control and TMD groups confirming the postulated significant difference regarding quantified symmetry comparison. (E) Bar chart of the statistical analyses between the control and TMD groups showing the smoothness of each specific opening or closing segment and the total trajectory. (F) Bar chart of statistical analyses between the control and TMD groups concerning separation for each trajectory. The bar charts indicate significant differences between the control and TMD groups. Black vertical lines show 95 % high-end threshold in normal population. * $P < 0.05$ denotes statistical significance, and ns indicates nonsignificant differences.

postoperative evaluations but also enhances postoperative outcome assessments of various treatment approaches, ultimately contributing to optimized patient care.

Although the binocular stereo system we developed is a specialized device, the underlying methodology can be adapted for use with commercially available 3D imaging and motion capture systems, which are becoming increasingly common in clinical practice. Many dental clinics already utilize advanced imaging technologies, such as CBCT and optical tracking systems, and our approach can be integrated with these existing tools through software adjustments and proper calibration. This minimizes the need for new hardware and maximizes the use of current resources, making the implementation both feasible and cost-effective. As the cost of high-quality imaging systems continues to decrease and further research advances, this methodology is expected to become more practical for routine clinical use.

This study has several limitations. First, the prefixed positioning of the binocular stereo cameras and jaw trackers may introduce variability in the results across different planes, necessitating future detailed and quantitative assessments of intra-operator and inter-operator reliability concerning the repeatability of marker positioning. Another limitation of our study is the inherent error associated with CBCT imaging in detecting landmarks and reference points due to the available voxel size of 0.3 mm. This voxel limitation may introduce minor inaccuracies in point localization, affecting the precision of motion trajectory analysis. Additionally, despite our efforts to mitigate the effects of velocity on computations through resampling during preprocessing, its impact on the rendered trajectories cannot be overlooked as a technical drawback. To address these limitations, future studies should aim to collect data from multiple motion cycles with sufficient interval times, as well as incorporate other mandibular motions, such as retrusion, protrusion, and lateral excursions, to assemble a more comprehensive and reliable dataset. Furthermore, integrating big data analysis and AI learning could facilitate identifying subtle patterns in mandibular motion across diverse populations and conditions, helping to define normative thresholds and TMD-related deviations more accurately. Nevertheless, the presented methodology complements current optical acquisition instruments such as Modjaw and SDiMatrix, which offer CBCT image fusion capabilities by integrating our data processing technique to visualize mandibular motion trajectories.

5. Conclusions

We conducted an in-depth quantitative characterization of mandibular movement features in both healthy individuals and those diagnosed with anterior disc displacement with reduction of the TMJ. This investigation provided a population-specific reference interval for smoothness, open-closure separation, and left-right symmetry and revealed substantial differences in all comparisons, suggesting its potential to distinguish patients with TMD from those with normal conditions in clinical assessments. From a clinical perspective, our findings were internally validated and aligned with the evaluations of clinical experts.

CRediT authorship contribution statement

Wen Tang: Writing – original draft, Methodology, Investigation, Formal analysis, Data curation, Conceptualization. **Yue Wu:** Investigation, Formal analysis, Data curation, Conceptualization. **Jiajun Ma:**

Software, Project administration, Methodology, Data curation. **Peter Svensson:** Visualization, Supervision, Methodology. **Kelun Wang:** Visualization, Supervision, Methodology. **Hengjia Zhang:** Validation, Supervision. **Lizhe Xie:** Visualization, Supervision, Methodology, Funding acquisition, Formal analysis, Conceptualization. **Bin Yan:** Writing – review & editing, Visualization, Supervision, Resources, Methodology, Funding acquisition, Conceptualization.

Declaration of competing interest

The authors declare that they have no known competing financial interests or personal relationships that could have appeared to influence the work reported in this paper.

Funding

This study was supported and funded by the National Natural Science Foundation of China (82371000, 82071143 and 82101079), the National Key Research and Development Program of China (2022YFC2402103 and SQ2023YFC2400025), and the Key R&D Program of Jiangsu Province (BE2022795 and BE2023836).

Ethics approval and consent to participate

The study design was approved by the National Chinese Clinical Trial Registry (ChiCTR) with approval number ChiCTR23000772980 and Nanjing Medical University institutional ethical review board with approval number PJ2022-110-001. All individual participants provided informed consent to participate in the study.

Availability of data and materials

The datasets generated and/or analyzed during the current study are not publicly available due to the confidentiality of patient images and parallel investigations pertaining to other research but are available from the corresponding author upon reasonable request.

Declaration of generative AI in the writing process

During the preparation of this work the authors used ChatGPT in order to improve the readability of this manuscript. After using this tool, the author(s) reviewed and edited the content as needed and take full responsibility for the content of the published article.

Acknowledgment

The authors extend their sincere gratitude to Rui Chen (School of Cyber Science and Engineering, Southeast University, China) as well as Libo Cao (Nanjing Medical University, China) for their contributions to data curation and validation. The authors also thank Iman Izadikhah (Nanjing Medical University, China) and Sherif Elbarbary (Restorative Dentistry Unit, School of Clinical Dentistry, University of Sheffield, Sheffield, United Kingdom) for their valuable efforts in reviewing and editing this research. Additionally, we sincerely appreciate Linlin Zhu and Li Hu (Nanjing Medical University, China) for their instrumental role in facilitating the participation of volunteers for this study. Lastly, we extend our heartfelt gratitude to all the volunteers who participated

in this project.

Supplementary materials

Supplementary material associated with this article can be found, in the online version, at doi:10.1016/j.jdent.2024.105534.

References

- [1] X. Xu, F. Song, L. Wu, L. Zhang, X. Liu, Investigation of the accuracy of dynamic condylar position: a model study, *J. Dent.* 143 (2024) 104889, <https://doi.org/10.1016/j.jdent.2024.104889>.
- [2] A.H. Alrizqi, B.M. Aleissa, Prevalence of Temporomandibular Disorders Between 2015–2021: a Literature Review, *Cureus* 15 (2023) e37028, <https://doi.org/10.7759/cureus.37028>.
- [3] F.P. Kapos, F.G. Exposto, J.F. Oyarzo, J. Durham, Temporomandibular disorders: a review of current concepts in aetiology, diagnosis and management, *Oral Surg* 13 (2020) 321–334, <https://doi.org/10.1111/ors.12473>.
- [4] D.V. da Cunha, V.V. Degan, M. Vedovello Filho, D.P. Bellomo, M.R. Silva, D. A. Furtado, A.O. Andrade, S.T. Milagre, A.A. Pereira, Real-time three-dimensional jaw tracking in temporomandibular disorders, *J. Oral Rehabil.* 44 (2017) 580–588, <https://doi.org/10.1111/joor.12521>.
- [5] Z. Khachatryan, T. Hambartsoumian, L. Tatintyan, S. Burnazyan, G. Hakobyan, Efficacy of the transcutaneous electrostimulation in treatment dysfunctions of the TMJ associated with occlusion distortions, *BMC Oral Health* 23 (2023) 937, <https://doi.org/10.1186/s12903-023-03662-z>.
- [6] E. Schiffman, R. Ohrbach, E. Truelove, J. Look, G. Anderson, J.-P. Goulet, T. List, P. Svensson, Y. Gonzalez, F. Lobbezoo, A. Michelotti, S.L. Brooks, W. Ceusters, M. Drangsholt, D. Ettlin, C. Gaul, L.J. Goldberg, J.A. Haythornthwaite, L. Hollender, W. Maixner, M. van der Meulen, G.M. Murray, D.R. Nixdorf, S. Palla, A. Petersson, P. Pionchon, B. Smith, C.M. Visscher, J. Zakrzewska, S.F. Dworkin, Diagnostic Criteria for Temporomandibular Disorders (DC/TMD) for Clinical and Research Applications: recommendations of the International RDC/TMD Consortium Network* and Orofacial Pain Special Interest Group†, *J. Oral Facial Pain Headache* 28 (2014) 6–27, <https://doi.org/10.11607/jop.1151>.
- [7] R. Ohrbach, S.F. Dworkin, The Evolution of TMD Diagnosis, *J. Dent. Res.* 95 (2016) 1093–1101, <https://doi.org/10.1177/0022034516653922>.
- [8] R. Bird, E.V. Beecroft, TMD diagnosis—What should general dentists and orthodontists know? *Semin. Orthod.* 30 (2024) 243–249, <https://doi.org/10.1053/j.sodo.2024.01.002>.
- [9] D. Singh, A. Landry, M. Schmid-Schwab, E. Piehlsinger, A. Gahleitner, J. Chen, X. Rausch-Fan, Clinical and MRI-Based Assessment of Patients with Temporomandibular Disorders Treated by Controlled Mandibular Repositioning, *Diagnostics* 14 (2024) 572, <https://doi.org/10.3390/diagnostics14060572>.
- [10] A. Sclaro, S. Khijmatgar, P.M. Rai, F. Falsarone, F. Alicchio, A. Mosca, C. Greco, M. Del Fabbro, G.M. Tartaglia, Efficacy of Kinematic Parameters for Assessment of Temporomandibular Joint Function and Dysfunction: a Systematic Review and Meta-Analysis, *Bioengineering* 9 (2022), <https://doi.org/10.3390/bioengineering9070269>.
- [11] M.O. Ahlers, O. Bernhardt, H.A. Jakstat, B. Kordaß, J.C. Türp, H.-J. Schindler, A. Hugger, Motion analysis of the mandible: guidelines for standardized analysis of computer-assisted recording of condylar movements, *Int. J. Comput. Dent.* 18 (2015) 201–223, <http://www.ncbi.nlm.nih.gov/pubmed/26389133>.
- [12] M.O. Ahlers, T. Petersen, L. Katzer, H.A. Jakstat, J.C. Roehl, J.C. Türp, Condylar motion analysis: a controlled, blinded clinical study on the interindividual reproducibility of standardized evaluation of computer-recorded condylar movements, *Sci. Rep.* 13 (2023) 1–14, <https://doi.org/10.1038/s41598-023-37139-4>.
- [13] P. Chantaracherd, M.T. John, J.S. Hodges, E.L. Schiffman, Temporomandibular Joint Disorders' Impact on Pain, Function, and Disability, *J. Dent. Res.* 94 (2015) 79S–86S, <https://doi.org/10.1177/00220345154565793>.
- [14] O. Leissner, M. Maulén-Yáñez, W. Meeder-Bella, C. León-Morales, E. Vergara-Bruna, W.A. González-Arriagada, Assessment of mandibular kinematics values and its relevance for the diagnosis of temporomandibular joint disorders, *J. Dent. Sci.* 16 (2021) 241–248, <https://doi.org/10.1016/j.jds.2020.05.015>.
- [15] A.A. Nigam, J.D. Lee, S.J. Lee, A clinical comparison of sagittal condylar inclination and Bennett angle derived from a conventional electronic tracking device and an optical jaw tracking device, *J. Prosthet. Dent.* (2023) 1–6, <https://doi.org/10.1016/j.prosdent.2023.10.034>.
- [16] M. Revilla-León, J.M. Zeitler, E. Fry, J.C. Kois, Digital workflow to measure the mandibular range of motion using different jaw tracking technologies, *J. Prosthet. Dent.* (2024) 1–8, <https://doi.org/10.1016/j.prosdent.2023.12.018>.
- [17] M. Revilla-León, D.E. Kois, J.M. Zeitler, W. Att, J.C. Kois, An overview of the digital occlusion technologies: intraoral scanners, jaw tracking systems, and computerized occlusal analysis devices, *J. Esthet. Restor. Dent.* 35 (2023) 735–744, <https://doi.org/10.1111/jerd.13044>.
- [18] S.C. Woodford, D.L. Robinson, A. Mehl, P.V.S. Lee, D.C. Ackland, Measurement of normal and pathological mandibular and temporomandibular joint kinematics: a systematic review, *J. Biomech.* 111 (2020) 109994, <https://doi.org/10.1016/j.jbiomech.2020.109994>.
- [19] A.A. Nigam, J.D. Lee, S.J. Lee, A clinical comparison of sagittal condylar inclination and Bennett angle derived from a conventional electronic tracking device and an optical jaw tracking device, *J. Prosthet. Dent.* (2023), <https://doi.org/10.1016/j.prosdent.2023.10.034>.
- [20] A. Choi, S.-B. Joo, E. Oh, J.H. Mun, Kinematic evaluation of movement smoothness in golf: relationship between the normalized jerk cost of body joints and the clubhead, *Biomed. Eng. Online* 13 (2014) 20, <https://doi.org/10.1186/1475-925X-13-20>.
- [21] M.F. Lezcano, F.J. Dias, P. Chuhuaicura, P. Navarro, R. Fuentes, Symmetry of mandibular movements: a 3D electromagnetic articulography technique applied on asymptomatic participants, *J. Prosthet. Dent.* 125 (2021) 746–752, <https://doi.org/10.1016/j.prosdent.2020.01.020>.
- [22] J. Shu, H. Ma, X. Xiong, B. Shao, T. Zheng, Y. Liu, Z. Liu, Mathematical analysis of the condylar trajectories in asymptomatic subjects during mandibular motions, *Med. Biol. Eng. Comput.* 59 (2021) 901–911, <https://doi.org/10.1007/s11517-021-02346-6>.
- [23] E. von Elm, D.G. Altman, M. Egger, S.J. Pocock, P.C. Gøtzsche, J. P. Vandenbroucke, The Strengthening of Reporting of Observational Studies in Epidemiology (STROBE) Statement: guidelines for Reporting Observational Studies, *Ann. Intern. Med.* 147 (2007) 573, <https://doi.org/10.7326/0003-4819-147-8-200710160-00010>.
- [24] J. Procházka, D. Martinek, Notes on iterative closest point algorithm, 17th Conf. in: *Appl. Math. APLIMAT 2018 - Proc. 2018-Febru, 2018*, pp. 876–884.
- [25] D. Patel, S. Upadhyay, Optical Flow Measurement using Lucas Kanade Method, *Int. J. Comput. Appl.* 61 (2013) 6–10, <https://doi.org/10.5120/9962-4611>.
- [26] M. Robinson, Anatomy and function of the eye, *Hum. Exp. Toxicol.* 11 (1992) 563–564, https://doi.org/10.5005/jp/books/11837_8.
- [27] Dynamic Time Warping, *Inf. Retr. Music Motion*, Springer Berlin Heidelberg, Berlin, Heidelberg, 2007, pp. 69–84, https://doi.org/10.1007/978-3-540-74048-3_4.
- [28] L. Li, H. Chen, Y. Zhao, Y. Wang, Y. Sun, Design of occlusal wear facets of fixed dental prostheses driven by personalized mandibular movement, *J. Prosthet. Dent.* 128 (2022) 33–41, <https://doi.org/10.1016/j.prosdent.2020.09.055>.
- [29] S.S. Azer, Simulating mandibular movements and articulator design, *J. Prosthet. Dent.* 129 (2023) 377–379, <https://doi.org/10.1016/j.prosdent.2023.01.015>.
- [30] H. Sepp, H. Vinkka-Puhakka, T. Peltomäki, Mandibular movements in children with deciduous and mixed dentition and in young adults with permanent dentition—The association between movements and occlusal traits, *Eur. J. Orthod.* 43 (2021) 338–345, <https://doi.org/10.1093/ejo/cjaa033>.
- [31] J.-L. Pépin, C. Letesson, N.N. Le-Dong, A. Dedave, S. Denison, V. Cuthbert, J.-B. Martinot, D. Gozal, Assessment of Mandibular Movement Monitoring With Machine Learning Analysis for the Diagnosis of Obstructive Sleep Apnea, *JAMA Netw. Open* 3 (2020) e1919657, <https://doi.org/10.1001/jamanetworkopen.2019.19657>.
- [32] K.J. Jeon, Y.H. Kim, E.-G. Ha, H.S. Choi, H.-J. Ahn, J.R. Lee, D. Hwang, S.-S. Han, Quantitative analysis of the mouth opening movement of temporomandibular joint disorder patients according to disc position using computer vision: a pilot study, *Quant. Imaging Med. Surg.* 12 (2022) 1909–1918, <https://doi.org/10.21037/qims-21-629>.
- [33] W.E. McDevitt, A.A. Warreth, Occlusal contacts in maximum intercuspation in normal dentitions, *J. Oral Rehabil.* 24 (1997) 725–734, <https://doi.org/10.1111/j.1365-2842.1997.tb00268.x>.
- [34] T.H. Farook, F. Rashid, M.K. Alam, J. Dudley, Variables influencing the device-dependent approaches in digitally analysing jaw movement—A systematic review, *Clin. Oral Investig.* 27 (2022) 489–504, <https://doi.org/10.1007/s00784-022-04835-w>.
- [35] N. Khare, S.B. Patil, S.M. Kale, J. Sumeet, I. Sonali, B. Sumeet, Normal Mouth Opening in an Adult Indian Population, *J. Maxillofac. Oral Surg.* 11 (2012) 309–313, <https://doi.org/10.1007/s12663-012-0334-1>.
- [36] C. Huang, X. Xu, L. Li, Y. Sun, C. Guo, Study on the reconstruction of a four-dimensional movement model and the envelope surface of the condyle in normal adults, *Br. J. Oral Maxillofac. Surg.* 60 (2022) 884–889, <https://doi.org/10.1016/j.bjoms.2021.08.006>.
- [37] D.G.E. Robertson, G.E. Caldwell, J. Hamill, Research Methods in Biomechanics, 2nd ed., 2014.
- [38] H.J. Woltring, K. Long, P.J. Osterbauer, A.W. Fuhr, Instantaneous helical axis estimation from 3-D video data in neck kinematics for whiplash diagnostics, *J. Biomech.* 27 (1994) 1415–1432, [https://doi.org/10.1016/0021-9290\(94\)90192-9](https://doi.org/10.1016/0021-9290(94)90192-9).
- [39] A. Dinsdale, Z. Liang, L. Thomas, J. Treleven, Are jaw range of motion, muscle function and proprioception impaired in adults with persistent temporomandibular disorders? A systematic review and meta-analysis, *J. Oral Rehabil.* 47 (2020) 1448–1478, <https://doi.org/10.1111/joor.13090>.
- [40] A. Sclaro, S. Khijmatgar, P.M. Rai, F. Falsarone, F. Alicchio, A. Mosca, C. Greco, M. Del Fabbro, G.M. Tartaglia, Efficacy of Kinematic Parameters for Assessment of Temporomandibular Joint Function and Dysfunction: a Systematic Review and Meta-Analysis, *Bioengineering* 9 (2022) 269, <https://doi.org/10.3390/bioengineering9070269>.
- [41] S.E. Widmalm, Y. Dong, B.X. Li, M. Lin, L.J. Fan, S.M. Deng, Unbalanced lateral mandibular deviation associated with TMJ sound as a sign in TMJ disc dysfunction diagnosis, *J. Oral Rehabil.* 43 (2016) 911–920, <https://doi.org/10.1111/joor.12446>.
- [42] L. Zhang, L. Shen, L. Zhang, C. Zhang, H. Wang, Dynamic 3D images fusion of the temporomandibular joints: a novel technique, *J. Dent.* 126 (2022), <https://doi.org/10.1016/j.jdent.2022.104286>.